



**Factors influencing peak summer surface water
temperature in
Canada's large lakes (Area \geq 100 km²)**

Journal:	<i>Canadian Journal of Fisheries and Aquatic Sciences</i>
Manuscript ID	cjfas-2017-0061.R2
Manuscript Type:	Article
Date Submitted by the Author:	06-Aug-2017
Complete List of Authors:	Minns, Charles; University of Toronto, Department of Ecology and Evolutionary Biology Shuter, Brian; University of Toronto, Department of Ecology and Evolutionary Biology; Ontario Ministry of Natural Resources, Aquatic Ecosystem Science Section Davidson, Andrew; Agriculture and Agrifood Canada Wang, Shusen; Natural Resources Canada, Canada Centre for Remote Sensing
Is the invited manuscript for consideration in a Special Issue? :	N/A
Keyword:	Canada, Large lakes, Surface temperature, REMOTE SENSING < General, MODELS < General

SCHOLARONE™
Manuscripts

Factors influencing peak summer surface water temperature in Canada's large lakes (Area $\geq 100 \text{ km}^2$)

Authors: Charles K. Minns^{1,2}, Brian J. Shuter^{1,3}, Andrew Davidson^{4,5} and Shusen Wang⁴

¹ Department of Ecology and Evolutionary Biology, University of Toronto, ON M5S 3G5,
Canada

² Great Lakes Laboratory for Fisheries and Aquatic Science, Fisheries and Oceans Canada, PO
Box 5050, 867 Lakeshore Road, Burlington ON L7R 4A6, Canada

³ Harkness Laboratory of Fisheries Research, Aquatic Ecosystem Science Section, Ontario
Ministry of Natural Resources, 300 Water St., Peterborough, ON K9J 8M5 Canada

⁴ Canada Centre for Remote Sensing, Natural Resources Canada, 588 Booth Street, Ottawa, ON,
Canada

⁵ Agriculture and Agri-Food Canada, 960 Carling Avenue, Ottawa, ON, K1A 0C6, Canada

Author to who all correspondence should be addressed. e-mail: ken@minns.ca

Coauthors email: brian.shuter@utoronto.ca; Andrew.davidson@agr.gc.ca;

shuwang@nrcan.gc.ca.

Running Head: Peak Surface Water Temperature in Canadian Large Lakes

Keywords: Canada, Large lakes, Surface water temperature, Remote sensing, Models.

Acknowledgements

Thanks to those colleagues at Canada Centre for Remote Sensing whose prior research and development work enabled the use of the 2001-2002 remotely sensed data. Thanks also to Carolyn N. Bakelaar at Fisheries and Oceans Canada, Burlington, for her skillful assistance with the GIS maps used to prepare the mask for Canada's large lakes. This study was made possible with funding from the Climate Change Action Fund, Fisheries and Oceans Canada, Canada Centre for Remote Sensing, and Ontario Ministry of Natural Resources.

Draft

1 Abstract

2

3 Seasonal water temperature data from 388 large Canadian lakes were used to develop improved
4 empirical tools for forecasting the impacts of climate change on the magnitude (T_P) and time of
5 occurrence (J_P) of annual peak surface water temperatures. Analyses of remotely-sensed open
6 water temperatures with sinusoidal models produced estimates of T_P and J_P predominately better
7 than other models. Those estimates were analyzed for lake and climate patterns. Linear mixed
8 effects regression produced a significant model of T_P with fixed positive effects for mean July
9 and annual air temperatures and lake perimeter, but negative effects with mean July and annual
10 % cloud cover, mean annual precipitation, range of monthly mean global clear-sky radiation,
11 area, and elevation. Subsets of the estimates with mean, maximum or Secchi depth values
12 produced similarly significant models with negative depth coefficients. J_P was relatively
13 invariant but small, significant lake and climate effects were detected. The best models identified
14 in our analyses will be useful tools for forecasting how climate change will alter aspects of the
15 limnetic seasonal water temperature cycle that strongly influence the species composition and
16 productivity of their fisheries.

17

18 **Introduction**

19 Canada's freshwaters are threatened by a wide range of human activities (Chu et al 2015;
20 Schindler 2001). The greatest threat, climate change (IPCC 2013), is likely to exacerbate the
21 impacts of other stresses and has already caused large changes, especially in northern regions of
22 Canada (Reist et al 2006). Using remote sensing observations of surface temperatures, Larouche
23 and Galbraith (2016) have demonstrated significant warming of Canada's coastal seas and its
24 largest inland lakes over the period 1985 to 2013. Warming is the strongest and most clearly
25 defined impact of climate change on lakes, influencing their biodiversity and biological
26 productivity, especially fish and fisheries (Lynch et al 2016; Hunt et al 2016). Canada's large
27 lakes account for most of its freshwater fisheries productivity and projected warming may lead to
28 large decreases in yield (Minns 2009). To assess the biological changes induced by warming,
29 models are needed to project how lake temperatures will respond to climate warming.

30 Many modelling options are available. Mechanistic models of the thermal regimes of
31 lakes have advanced considerably with 2- and 3-D models (Patterson *et al* 1984; Blenckner *et al*
32 2002; Huang *et al* 2010). Many features of seasonal temperature dynamics can be simulated
33 using detailed temporal records of climate variables such as air temperature, solar radiation,
34 precipitation, and wind, along with lake morphometry. However, fitting these models can require
35 considerable time, data and computing resources and often require site-specific fine-tuning to
36 match observations (Tanentzap et al 2007). Typically, mechanistic models are applied to single,
37 large lakes and, overall, the effort and data requirements limit the use of such models for many
38 Canadian lakes particularly those in remote areas.

39 Semi-mechanistic and empirical models of lake temperatures typically result from
40 localized studies e.g., Scandinavia (Håkanson 1996); north central Ontario (Gunn et al 2001);
41 and the Swiss alpine region (Livingstone et al 2005). More extensive studies were reported by
42 Shuter et al (1983) for a mixed sample of Ontario and global lakes and by Sharma et al (2007)
43 for a large sample of *in situ* observations from Canadian lakes. Large lakes, of which Canada
44 holds the largest global share (Minns 2009), have been under-represented in previous semi-
45 mechanistic and empirical modelling efforts.

46 Remote sensing (RS) data are widely used to estimate surface water temperatures though
47 in freshwaters these studies are typically restricted to larger lakes because of factors related to
48 imagery pixel sizes and resulting edge effects at land-water boundaries (Gholizadeh et al 2016).
49 However, Bussièrès et al (2002) and Bussièrès and Schertzer (2003) showed that RS data could
50 be used to study surface temperatures in groups of Canadian lakes as small as 22 km². Wider use
51 of RS data will help elucidate the influence of various lake and climate metrics and further the
52 development of useful empirical models for predicting surface temperatures of large lakes. Given
53 the great span of warm to cold climates encountered over Canada's many large lakes, it should
54 be possible to mobilize RS data available for these systems to develop an empirical model of
55 climatic effects on lake water temperatures where space effectively substitutes for time. Such an
56 empirical model would permit freshwater scientists to assess how ongoing and projected future
57 climate change might influence the impacts of the many stressors (e.g., excess nutrients, invasive
58 species and exploitation) that continue to disrupt limnetic ecosystems across North America.

59 The objectives of this study were to: (1) model open-water surface water temperature
60 patterns observed in Canada's large lakes using remote sensing observations to estimate peak
61 summer surface temperature (T_P) and its date of occurrence (J_P), and (2) examine the relationship

Minns et al

CJFAS2017_0061 T_P J_P

21/06/2017

62 of those indicator metrics to lake morphometry and climate metrics. Peak, or maximum, surface
63 water temperature is a key predictor of mean surface temperature during the ice-free period in
64 lakes (Shuter et al 1983). It links with lake morphometry (e.g., lake area, maximum depth) to
65 determine the availability of suitable habitat space to support survival and productivity (Minns et
66 al 2014) of distinct thermal guilds of freshwater fishes (Hasnain et al 2013).

67 **Materials and methods**

68 **Data**

69 Remotely sensed (RS) data: As part of a collaborative study, the Canada Centre for Remote
70 Sensing (CCRS) provided us with the RS MODIS and AVHRR satellite data needed to examine
71 the seasonal surface temperature cycles for over 550 large lakes across Canada for the years 2001
72 to 2002. Skin temperatures were assembled for Canadian large lakes (Area $\geq 100 \text{ km}^2$) from
73 MODIS/Terra Land Surface Temperature (MOD11A1) and Albedo (MOD43B3) datasets for
74 2001 and 2002. Skin temperature refers to that detected by satellites in the first few millimetres
75 of surface waters while bulk temperature refers to that measured in the waters centimeters to
76 metres below the surface (Fairall et al 1996); limnologists generally consider the latter to be the
77 temperature experienced by fish and other biota. Daytime freshwater surface pixels were
78 aggregated into large lake polygons. After application of quality control criteria, a mean lake skin
79 temperature was computed. Ice break-up and freeze-up dates were derived from AVHRR remote
80 sensing data using the protocol of Latifovic and Pouliot (2007). Only usable daytime values
81 occurring during the open water season were subjected to further analysis. Out of 563 large
82 lakes identified (Figure 1), daytime skin temperature datasets were obtained for 554 lakes in
83 2001 and /or 2002. [See Appendix A for further details on skin temperature data assembly.]

84 Skin-to-bulk adjustment of temperatures: We used published NOAA GLSEA daily mean
85 surface temperatures based on a combination of remotely sensed and *in situ* data from the four
86 Canadian Great Lakes (Schwab et al. 1999; <https://coastwatch.glerl.noaa.gov/statistic/> as of
87 2017/06/04) to develop mixed effects regression model to make skin to bulk temperature
88 adjustments (See Appendix B for details).

89 Climate data: Monthly mean measures of air temperature (°C), precipitation (mm.d⁻¹),
90 and cloud cover (%) for 2001 and 2002 were extracted from the global 0.5° gridded CRU TS
91 v3.23 data base (see Harris et al 2014 for details); data were downloaded from the Centre for
92 Environmental Data Analysis at <http://www.ceda.ac.uk>) and extracted for the grid centroid
93 nearest the latitude-longitude centroid for each lake.; the lake-to-grid centroid distances ranged
94 from 0.6 to 31.2 km.

95 In addition, hourly global clear sky ground level solar radiation was estimated at each
96 lake site using the algorithm of Bird and Hulstrom (1981) using their recommended air
97 transmission coefficients at all sites. The hourly radiation values were summarized as monthly
98 means (R, W.m⁻²) and then Kasten and Czeplak's (1980) empirical model (Cloud-corrected
99 radiation $CR = R \cdot (1 - 0.75 \cdot (C/100)^{3.4})$) was used to adjust monthly mean radiation values for site-
100 specific differences in percentage cloud cover (C, %).

101 Summer and annual means for climate variables were computed from monthly values.
102 For each lake-year dataset, the mean July (JUL), summer (June-July-August, SUM), and annual
103 (ANN) values for temperatures (T, °C), total precipitation (P, mm), and cloud cover (C, %) were
104 selected for use in modelling of T_P and J_P values. For clear sky radiation (R, W.m⁻²) and cloud
105 corrected radiation (CR, W.m⁻²), the July (JUL) and annual (ANN) means were used along with
106 the annual range of monthly means (RGE). Examples of the notation used to reflect this are:

Minns et al

CJFAS2017_0061 T_P J_P

21/06/2017

107 T_{SUM} = mean summer air temperature; CR_{RGE} = the annual range of monthly cloud-corrected
108 solar radiation means.

109 Large lake physical data: The lake morphometry and Secchi depth data assembled by
110 Minns (2010) were used to describe physical characteristics of the lakes included in the RS data
111 base.

112 **Statistical analyses and modelling**

113 The analysis of lake open water surface temperatures had two components: 1) Modelling
114 seasonal open water surface temperature models to derive estimates of T_P and J_P; and 2) Analysis
115 of lake and climate factors affecting peak surface temperature (T_P) and its date of occurrence
116 (J_P). All statistical computing and plot preparation were performed using R (R Core Team 2015).
117 Where variables were log-transformed, natural logarithms (ln) were used throughout.

118 Linear regression modeling was used throughout as Sharma et al (2008) found that it
119 performed best in a comparison of four modeling methods applied to lake surface temperature
120 data. Where random effects were expected, linear mixed effects (LME) models were used (Zuur
121 et al 2009). All statements of statistical significance are for probability (*P*) <0.01 unless
122 otherwise stated. Best fit model selection was decided using the minimum corrected Akaike
123 Information Criterion (AIC_C; Anderson 2008, Burnham and Anderson 2004). AIC_C differences >
124 2 indicated models with substantially less support than selected 'best' models. Goodness of fit
125 was assessed using the index of variance explained (R²) for ordinary linear models and the
126 marginal and conditional equivalents (R²_M and R²_C) developed by Nakagawa and Schielzeth
127 (2013) for linear mixed-effects using the *sjmisc* R package of Lüdecke (2016).

128 Model selection to describe seasonal open-water temperature patterns in individual lakes:

129 Various empirical models of lake open water surface temperatures as a function of day of year

130 have been used. Quadratic polynomials have been used often (Shuter et al 1983; Sharma et al
131 2007; and Bussi eres et al 2002). Minns and Shuter (2013) fitted a linear break-point model where
132 surface temperature rises linearly to a mid-summer maximum and then declines linearly in a
133 seasonal temperature profile model. Although the annual patterns of solar radiation and air
134 temperature follow sinusoidal cycles (Stine et al 2011) few models based on sinusoidal functions
135 have been reported until recently (e.g., Toffolon et al 2014; Flaim et al 2016).

136 We initially considered six open water surface temperature model: quadratic, break-point
137 and a series of four sinusoidal forms. Each form has the advantage that a summer peak date (J_P)
138 can be identified when the surface temperature reaches a maximum (T_P). The term "Peak" is
139 defined here as the highest estimated temperature obtained with the fitted regression model. This
140 estimate of T_P should be relatively free of the noise associated with single point in time estimates
141 of the adjusted-skin temperature and more representative of the sustained maximum bulk water
142 temperature. In exploratory analyses, we found that one of the sinusoidal models generally
143 provided a better fit than the quadratic and breakpoint models. Quadratic models tended to be
144 flatter in mid-season, yielding lower T_P estimates while break-point T_P estimates were often
145 influenced by mid-season high outliers. J_P estimates tended to be similar regardless of model.

146 Sinusoidal models can be fit by non-linear least squares regression but here we chose the
147 alternative sine-cosine pair form (Stolwijk et al 1999) which is a transformation of a single sine
148 or cosine term and can be fit using linear regression. We examined four forms of the sinusoidal
149 model. In the first order model, an annual wavelength is used, assuming a symmetric annual
150 cycle, and in higher order models additional sine-cosine pairs are added with longer wavelengths
151 (integer multiples of day of year) to allow for any asymmetry within the annual cycle:

Minns et al

CJFAS2017_0061 T_P J_P

21/06/2017

152 $T_J = \beta_0 + \sum^n (\beta_{Si} \sin(i \cdot J \cdot \pi / 182.5) + \beta_{Ci} \cos(i \cdot J \cdot \pi / 182.5))$ where T_J is the surface
153 temperature (°C) on day of the year J , i is 1 to n and n is 1,2,3, or 4. In each model, the fitted
154 equation can be solved to provide estimates of T_P and J_P . The best sinusoidal fit was selected
155 using AIC_C. Each lake-year dataset was modelled separately using least squares regression.

156 We then fit the sinusoidal models to our full set of RS datasets. To identify usable
157 individual lake-year regression results for inclusion in succeeding analyses of variation in T_P and
158 J_P estimates, we applied four stringent quality control criteria: (1) A minimum dataset size of 25
159 open water lake average temperature values was required to reduce the potential impact of
160 outliers on the model fits and subsequent indicator estimates; (2) To ensure a higher likelihood of
161 finding the midsummer peaks expected to occur in the vicinity of day 200, only datasets with a
162 minimum day of year ≤ 180 and a maximum day of year ≥ 260 were retained to ensure that the
163 peak period was covered; (3) The best fit (minimum AIC_C) among the 1st to 4th order sinusoidal
164 models was selected; and (4) Following Prairie (1996), we only retained models with a goodness
165 of fit R^2 (Index of determination) ≥ 0.65 to ensure that we only used pairs of (T_P , J_P) estimates
166 derived from data sets where the seasonal pattern dominated over random variability.

167 Analysis of lake and climate factors affecting peak temperature (T_P) and its day of
168 occurrence (J_P): Usable T_P and J_P estimates were combined with appropriate lake specific
169 characteristics (ln-transformed values for area km², perimeter km and elevation above sea level
170 m, with 1 added to elevation to allow for sea level values) and year-specific climate data: July,
171 summer and annual mean air temperatures (T_{JUL} , T_{JJA} and T_{ANN}), total precipitation rates (P_{JUL} ,
172 P_{JJA} and P_{ANN}), and mean percentage cloud cover (C_{JUL} , C_{JJA} and C_{ANN}) from the nearest CRU
173 grid, along with the July, annual, and range of monthly mean solar radiation estimates for clear
174 sky (R_{JUL} , R_{ANN} and R_{RGE}), and cloud-corrected conditions (CR_{JUL} , CR_{ANN} and CR_{RGE}). Latitude

175 and longitude were not used as input variables as their values clearly followed gradients in
176 climate variables (Supplementary Figure S1). Maximum likelihood multiple linear regression
177 was used to assess the influence of lake and climate variables on peak skin temperatures. Mixed
178 effects models were applied using the *lme* function in the *nlme* R package (Pinheiro et al 2016).
179 Year, Lake, and Model (i.e. the sinusoidal form selected) were specified as potential random
180 intercept effects and the procedures outlined in Zuur et al (2009) were used for model selection.

181 For the subsets of the estimates where either maximum depth (Z_{MAX}), mean depth
182 (Z_{MEAN}) or Secchi depth (Secchi) values were available, additional LME modelling was
183 performed to assess the improvement in fit when each depth variable (ln-transformed) was
184 added. The net benefit of each depth variable was assessed using AIC_C differences to compare
185 the best subset model with depth included versus that model without depth included.

186 Additional ordinary least squares linear regressions were performed using Minns' (2010)
187 Canadian large lake dataset to assess relationships among perimeter, area, each of the depth
188 variables, and primary watershed membership (Minns 2008).

189 **Comparison with Previous Models of Peak Temperature**

190 Shuter et al. (1983) and Sharma et al. (2007) published empirical models for predicting
191 peak summer temperatures. The former used data from Ontario and elsewhere around the world
192 while the latter used data from all regions of Canada. Those models were used to predict
193 comparison values for our estimates of T_P .

194 From Shuter et al (1983) we used their model 10 (Shuter et al 1983 Table 4) using mean
195 lake depth:

$$196 \quad T_P = \exp(3.059 + 0.0422 * T_{ANN} - 0.002 * T_{ANN}^2 - 0.01 * (\ln Z_{MEAN})^3 + 0.062).$$

Minns et al

CJFAS2017_0061 T_P J_P

21/06/2017

197 The +0.062 term is the residual standard deviation that provides the log-transformation bias
198 correction (Sprugel 1983). To predict missing Z_{MEAN} values, we used the best predictive
199 equation ($F_{\text{REGR}} = 48.44$ on 3,150 d.f., adj. $R^2 = 0.482$, residual std. error = 0.742, $P < 0.001$) for
200 $\text{Ln } Z_{\text{MEAN}}$ derived from our analyses of lake physical data in the Minns (2010) large Canadian
201 lake data base:

202 $\text{Ln } Z_{\text{MEAN}} = +0.0561 + 0.4929 * \text{Ln Perimeter}$ if PWS = 1,2, or 10, and modified by
203 -0.8073 if PWS = 3,4,5,6, or 7 or $+1.2939$ if PWS = 8 or 9.

204 PWS stands for primary watershed code (Minns et al 2010). Canada's largest watersheds
205 were designated as PWS representing major physiographic regions: PWS = 1,2, and 10
206 refer to the Maritime provinces, St. Lawrence-Great Lakes, and Arctic basins
207 respectively; 3 to 7 refer to the basins draining into the Arctic Ocean (Northern Quebec
208 and Labrador, S. Hudson Bay, Nelson R., W. & N. Hudson Bay, and Great Slave Lake
209 respectively); and 8-9 refer to basins draining into the Pacific Ocean (Pacific coast, and
210 Yukon R. respectively).

211 Sharma et al (2007) developed two regression models to predict maximum summer
212 surface temperature in Canadian lakes:

213 $\text{Model 1} = -57.88 + 0.79 * T_{\text{JUL}} + 0.26 * T_{\text{ANN}} + 0.617 * J - 0.00151 * J^2 - 0.019 * \text{Lon} + \beta_1$

214 $\text{Model 2} = -44.72 + 0.76 * T_{\text{JUL}} + 0.59 * J - 0.0015 * J^2 - 0.034 * \text{Lon} - 0.23 * \text{Lat} + \beta_2$

215 Where, Lon is ° longitude, Lat is ° latitude, and β_1 and β_2 are year-specific coefficients (values
216 for 2001 and 2002 were reported in Appendix A of Sharma et al 2007). The models' peak dates,
217 i.e. J_p values, (204.3, 196.7 respectively) reported by Sharma et al. were used to make peak
218 predictions. The average of the two models' predictions was used here.

219 **Results**

220 **Lake-wide Mean Surface Temperatures**

221 Overall there were 77,624 daily RS average lake skin temperature values spread across
222 1064 lake-year datasets with sample sizes of 9 to 198 (median 69). Across these data sets, the
223 earliest day of year spanned from 36 to 231 (median 148) while the latest spanned from 223 to
224 365 (median 317). Apart from a few extreme outliers 90% of the maximum skin temperatures lay
225 between 13.8 and 29.9 °C with 90% of those values occurring between days 179 and 228. No
226 data points were excluded from the analyses that follow.

227 The GLSEA-based skin-to-bulk adjustment model resulted in a median difference
228 (GLSEA bulk – our adjusted RS) of +0.23C with the 10th and 90th percentiles at 2.82 and +2.57C
229 respectively. Further, preliminary seasonal modelling with the Great Lakes datasets showed that
230 T_P and J_P estimates obtained with daily open water GLSEA bulk temperatures and our less
231 frequent adjusted RS data were similar with comparable high R² values and that sinusoidal
232 equations provided the best models in most cases. (See Appendix B for details about the
233 adjustment models and Great Lakes seasonal model selection).

234 **Seasonal Model Selection for All Lake Datasets**

235 There were 1064 lake-year adjusted-RS temperature datasets. The best fit sinusoidal
236 model was identified for each dataset and, after applying our quality control criteria, (i.e., sample
237 size, date range, and R²) 690 usable estimates of T_P and J_P were identified. Estimates based on
238 the quadratic model were on average 0.93 (SD 0.87) °C below and 0.2 (SD 10.7) days later than
239 the selected sinusoidal predictions while breakpoint estimates were on average 2.54 (SD 1.31) °C
240 above and 1.3 (SD 13.4) days earlier. These differences of the quadratic and breakpoint estimates

241 from the best sinusoidal ones are in the expected directions and are relatively small, suggesting
242 that our (T_P, J_P) estimates are relatively robust to the specific model used in their estimation.
243 Among our 690 results, the 1st order sinusoidal model was best in 594 cases, the 2nd order in 89,
244 and the 3rd order in 7. The estimates came from 302 lakes present in both years and 51 and 35
245 additional lakes present only in 2001 and 2002 respectively. We selected the lowest AIC_C among
246 the preferred sinusoidal model fits as the reference AIC_C for assessing model fit differences. If a
247 quadratic or breakpoint model AIC_C was lower than the minimum sinusoidal model AIC_C, the
248 AIC_C difference was shown as negative, with values < -2 indicative of a better fit. With the
249 quadratic model the AIC_C difference (relative to the best sinusoidal model) was between +2 and
250 -2 in 60 cases indicating a comparable fit, and less than -2 in 20 cases, indicating a better fit,
251 whereas with the break-point model the AIC_C difference was between +2 and -2 in 107 cases
252 indicating a comparable fit, and less than -2 in 123 cases indicating a better fit. Since sinusoidal
253 models gave the best fit most often and since this equation form was most consistent with the
254 expected seasonal solar and air temperature cycles, we chose to base our analysis of variation in
255 T_P and J_P using estimates derived from the best sinusoidal models.

256 To demonstrate results obtained with alternate models, nine lake-year datasets were
257 selected based on the best sinusoidal model across the range of R² obtained from 0.69 to 0.91
258 (Figure 2; lake details are given in Supplementary Table S1). The plots of the data and the
259 predicted curves for the best sinusoidal, the quadratic, and the break-point models show how the
260 breakpoint estimates of T_P were generally higher than the best sinusoidal estimate and the
261 quadratic model estimates were lower. The sinusoidal models follow the overall patterns of
262 observations better than the quadratic and breakpoint models and provide the basis for deriving
263 estimates of T_P and J_P unaffected by outliers (Figure 2).

264 Analysis of Lake and Climate Factors Affecting T_P and J_P

265 The 690 usable estimates of T_P and J_P were not correlated ($R^2 = 0.01$) and had mean
266 values of 18.8 (SD 3.1) °C and 205.9 (SD 7.2) days for T_P and J_P respectively (See Table S2 for
267 a full summary of these estimates and associated lake and climate variables). Univariate plots of
268 T_P and J_P against climate and lake metrics revealed some strong associations (Figures 3 and 4;
269 Supplementary Figures S2 and S3). With respect to climate (Figure 3), peak temperature (T_P)
270 increased with increases in all three mean air temperature metrics; increased with increases in
271 four of the radiation metrics, mean July clear sky, annual clear sky and their cloud-corrected
272 versions; decreased with July and summer mean percent cloud cover and the range of monthly
273 mean clear sky radiation; and showed no clear trends with the remaining climate metrics. With
274 respect to lake metrics (Figure 4), T_P decreased with increases in lake area, the three depth
275 metrics and latitude; and showed a humped-shaped relationship with longitude. The less-variable
276 date of occurrence (J_P) increased with increases in lake area, perimeter, and the depth metrics
277 (Supplementary Figure S2); but exhibited less distinct patterns with climate metrics
278 (Supplementary Figure S3).

279 The multivariate regression modelling results were more revealing. Best fit LME
280 modelling of our 690 usable T_P and J_P estimates produced significant results (Table 1). With T_P,
281 the R^2 values were high with most of the variance attributable to the fixed effects ($R^2_M = 0.74$ vs.
282 $R^2_C = 0.93$) and with several fixed variables being included in the model. The random effects
283 variation due to the sinusoidal model selected and lake were similar in size to the residuals.
284 Among the fixed effects, area and perimeter were both included with opposite signs. Elevation
285 contributed a negative effect. Among the climate variables, T_{JUL} and T_{ANN} exerted positive
286 effects while P_{ANN}, C_{JUL}, C_{ANN}, and R_{RGE} exerted negative effects. Most of the variance in the

287 best fit model for J_P was attributable to the random effects ($R^2_M = 0.29$ vs. $R^2_C = 0.80$), while the
288 fixed variables that were included in the model indicated lake shape and landscape position as
289 having some influence.

290 LME modelling of the subsets of lakes where depth information was available yielded
291 results that strongly supported inclusion of depth variables in best-fit models: AIC_C differences,
292 between the best fit model with the depth variable included and the same model except that the
293 depth variable was removed, ranged from 32.6 (T_P with Ln Secchi) to 86.9 (J_P with Ln Z_{MEAN})
294 (Table S3). With T_P and J_P, inclusion of any depth variable led to the exclusion of elevation as a
295 predictor variable. In models of T_P, depth slopes were negative (e.g. slopes for Ln depth ranged
296 from -0.72 to -0.91); in J_P models, depth slopes were positive (e.g. slopes for Ln depth ranged
297 from 1.99 to 2.91). With T_P and J_P, the Ln area and Ln perimeter variables were both included in
298 all best fit models with similar magnitudes and opposite signs; larger areas made the timing of
299 peak occurrence (J_P) later and peak temperature (T_P) lower while longer perimeters made J_P
300 earlier and T_P higher. With T_P, the pattern for climate variables included in the best fit model
301 was similar, no matter which depth variables were included, T_P increased with air temperature
302 and annual clear sky radiation and decreased with precipitation, cloud cover and cloud-corrected
303 radiation. With J_P, fewer climate variables were included in the best fit models: T_{SUM} had a
304 positive effect in the models that included maximum and mean depth; C_{JUL} and R_{JUL} had positive
305 effects when maximum depth was included; R_{ANN} and R_{RGE} had negative effects with maximum
306 depth; and R_{RGE} had negative effects with mean and Secchi depths.

307 To clarify the opposing signs of lake area and perimeter coefficients in the best J_P and T_P
308 models, regression models were fitted between Ln perimeter and Ln area for Minns' (2010) large
309 lakes dataset (Supplementary Table S4). Overall, Ln area was a good predictor on average of Ln

310 perimeter ($R^2 = 0.65$ with a slope coefficient of +0.58). By substituting the area coefficient from
311 the perimeter vs area regression model for the corresponding perimeter coefficients in the J_P and
312 T_P models (Table 1) the net overall effect of ln area, on average, can be estimated. For J_P, the net
313 area coefficient was 2.64 indicating a later peak date of occurrence with larger areas. For T_P, it
314 was -0.92 indicating lower peak temperatures with larger areas. Further, when actual perimeter
315 values are greater than regression-predicted values for a given area, predicted J_P will be earlier
316 and predicted T_P higher; when actual perimeter values are lower than regression-predicted
317 values, J_P will be later and T_P lower.

318 **Comparison with Previous Models of Peak Summer Temperature**

319 T_P values predicted using the Shuter et al. (1983) model 10 and the average of the
320 Sharma et al. (2007) models 1 and 2 were comparable to our estimates ($R^2 = 0.51$ and 0.64
321 respectively, Figure 5). The Shuter et al. model predictions were generally higher than our
322 estimates and points based on estimated Ln Z_{MEAN} values were predominant at lower T_P values
323 as expected since more remote, northerly lakes are less likely to have depth data (Figure 5A).
324 With the mean of the Sharma et al models, the estimate-prediction points were uniformly
325 distributed along but mainly below the 1:1 line and the 2001 and 2002 point distributions
326 overlapped (Figure 5B). On average, our estimates were -2.54 °C (SD 2.40) lower than the
327 Shuter et al. predictions while our estimates were -1.05 °C (SD 1.87) lower than the average of
328 Model 1+2 predictions of Sharma et al. In addition, Sharma et al.'s two estimates of peak timing
329 (J_P) were similar the mean of our estimates 204.3 and 196.7 vs 205.9 (SD 7.2).

330 **Discussion**

331 Our analyses of adjusted RS lake surface temperature data allowed us to develop models
332 showing the influence of lake and climatic variables on peak summer surface temperature (T_P)
333 and its date of occurrence (J_P) in Canadian large lakes. The steps in the analyses are examined
334 before interpreting the models and comparing them with previous studies.

335 **Data analysis and modelling**

336 Two components of the data analysis need examination: (i) best fit model selection to
337 describe seasonal open water surface temperature patterns; and (ii) analysis of the effect of lake
338 and climate metrics on peak temperature and its date of occurrence.

339 **Model equation selection**

340 Given (i) the *a priori* expectation that surface water temperatures, like solar radiation and
341 air temperatures, will follow sinusoidal cycles (Brock 1981; Stine et al 2011; Henderson-Sellers
342 1986; Toffolon et al 2014), (ii) the repeated observation of such patterns in field data, and (iii)
343 the generally superior performance of sinusoidal models: such models should be preferred for
344 characterizing lake surface temperature patterns during the open water season. Overall, the best
345 fit sinusoidal models performed better in our analyses than the quadratic and breakpoint
346 alternatives. With selected models, the 1st sinusoidal model was typically best for northern lakes
347 with shorter open water seasons (Mean latitude °: 1st 54.4, 2nd 54.1, and 3rd 49.5). The 1st
348 sinusoidal model was also selected more often in lakes with fewer data values (Mean sample
349 size: 1st 82, 2nd 96, and 3rd 106) thereby limiting the ability to discern more complex seasonal
350 patterns inherent in higher order models.

351 Factors Affecting T_P and J_P in Large Lakes

352 The best T_P models included mixtures of lake and climate variables. Arhonditsis et al
353 (2004) showed that air temperature and incident solar radiation are the dominant physical
354 processes forcing thermal regimes in lakes. Air temperature is directly involved as air and
355 surface waters exchange heat. Air temperature metrics were included in the overall models as
356 well as in the models that included depth values. Incident radiation was represented directly by
357 clear-sky or cloud-corrected metrics and indirectly by precipitation and cloud cover.

358 The consistent inclusion of both area and perimeter in all the best fit models was
359 unexpected given the high correlation between the lake dimensions but a robust result
360 nonetheless. The comparative fitting procedure with the depth subsets showed consistently that
361 adding a depth variable always markedly improved the model fit. The depth variables themselves
362 are correlated (Minns 2010) and increased depth is expected to result in lower peak temperatures
363 and delay the peak date of occurrence (Arhonditis et al 2004). The effects of lake area, perimeter,
364 and depth on the peak temperature indicators are inter-twined. Our T_P estimates showed good
365 overall agreement with predictions derived from the models of Shuter et al (1983) and Sharma et
366 al (2007). Those models were primarily developed using observations from groups of lakes
367 smaller than those used in our study ($\geq 100 \text{ km}^2$). Peak temperatures are expected to be lower in
368 larger, deeper lakes (Arhonditsis et al 2004). Z_{MEAN} had a negative effect on the Shuter et al
369 model while no lake size variables were included in the Sharma et al models. The Shuter et al
370 model was developed with far fewer data (87 North American regional lakes and 25 lakes local
371 to S. Ontario) and with mostly smaller lakes than our model and hence may be less reliable when
372 used to predict values in larger lakes across Canada.

373 The net effect on T_P of ln area after adjustment for perimeter (Table S3) was negative
374 with slopes of -0.64 to -0.95 depending on whether and which depth variable (slopes -0.97 to –
375 0.69) was included. This effect likely reflects the role of lake depth, as the energy required to
376 fully mix and heat or cool a lake increases with depth (Hondzo and Stefan 1993), and mean and
377 maximum depths are strongly positively correlated with lake area (Minns et al 2008). The
378 positive effect of lake perimeter on T_P probably reflects the degree to which the lake surface is
379 effectively divided into a series of smaller water bodies with some inshore areas behaving more
380 like small shallow lakes (Chubarenko and Hutter 2005). Elevation was included in the overall T_P
381 model consistent with the observations of Livingstone et al (2005) who have shown in Swiss
382 alpine lakes that differences in altitude affect the impact of air temperature on lake temperatures.
383 Gunn et al (2001) showed that higher DOC levels were accompanied by small increases in late
384 summer surface temperatures (0.36 °C per mg. L⁻¹) in a series of dilute Ontario lakes. DOC
385 strongly affects light penetration in lakes and thus influences mixing and stratification depths
386 (Snucins and Gunn 2000). Consistent with these DOC effects, our best subset model for T_P
387 included Secchi depth (a strong correlate of DOC) with a slope of -0.85.

388 The relatively invariant date of occurrence of the peak surface water temperature J_P
389 (Mean = 205.9 ± SD 7.2) is consistent with the annual solar radiation cycle; J_P comes on day 206
390 or 24 days after summer solstice, (June 21 or day 182), a lag consistent with that in air
391 temperatures over land of 29 days (Stine et al 2011). The low fixed effect R² values for J_P models
392 are most likely explained by lake-specific variation in shape, surrounding landscape conditions,
393 and elevation contours.

394 The latitudinal and longitudinal effects included in the Sharma et al (2007) models
395 provided surrogates for factors affecting incident solar radiation inputs included directly in our

396 models. Latitude can serve as a surrogate for incident solar radiation as shown empirically for
397 Canadian sites by Yin (1996). Regional cloud cover patterns are consistent with the expected
398 effects of continentality (Currey 1974) where midcontinent climates have less cloud cover and
399 greater annual temperature extremes than coastal ones with the oceans exerting a moderating
400 effect. Midcontinent maximum lake surface temperatures are predicted to be higher than coastal
401 ones.

402 Our peak temperature models predict a 0.32-0.61 °C increase given a simultaneous 1 °C
403 increase in all the air temperature metrics (T_{JUL} , T_{SUM} , T_{ANN}). This range of rates is consistent
404 with the average observed temporal rates (0.36 and 0.55 °C. decade⁻¹) reported by O`Reilly et al
405 (2015) for groups of lakes spanning the main region of Canadian large lakes, and shown recently
406 for the Great Lakes by Larouche and Galbraith (2016). The climate warming implications are
407 clear; for every 1 °C increase in annual mean air temperature we can expect peak midsummer
408 lake temperatures to rise by ~0.45 °C. Further analysis of large lake temperatures gathered
409 routinely via remote sensing data should help document the regional patterns of warming across
410 Canada's freshwater resources.

411 Lakes integrate the effects of climate warming (Williamson et al 2009). Remote sensing
412 can provide near-continuous monitoring of surface water temperatures in Canada's large lakes
413 (Latifovic et al 2005) as demonstrated for the Great Lakes by Larouche and Galbraith (2016),
414 Such monitoring may require periodic calibration with *in situ* observations as satellite platforms
415 change and sensors age (Schwab et al 1999; Wang et al 2012). Lakes smooth out the variability
416 present in atmospheric observations (Williamson et al 2009). Lake surface water temperatures,
417 and associated phenomena such as ice formation and breakup and stratification, are the primary
418 determinants of the biological dynamics occurring in lakes (Shuter et al 2012). Hence tools that

Minns et al

CJFAS2017_0061 T_P J_P

21/06/2017

419 forecast how these characteristics will change for Canada's large lakes have significant practical
420 value, particularly for northern lakes where background data is very sparse (Minns et al 2008,
421 Minns 2010). Overall the models developed here for peak summer surface temperature and its
422 date of occurrence (T_P, J_P) highlight the simplicity of the relationships that link surface
423 temperature patterns to climate and morphometry in Canadian lakes, relationships that are
424 consistent with expectations from the basic physical processes embodied in mechanistic models
425 of lake thermal regimes (Henderson-Sellers 1986; Arhonditsis et al 2004). These models should
426 enable more detailed regional assessments (Minns et al 2008; Minns 2010) of the potential
427 impacts of climate change and the cumulative impacts of other stressors on Canada's freshwater
428 resources and their biota.

Draft

429 **References**

- 430 Anderson, D.R. 2008. *Model Based Inference in the Life Sciences: A Primer on Evidence*.
431 Springer Science+Business Media, New York, New York. 184p.
- 432 Arhonditsis, G.B., Brett, M.T., De Gasperi, C.L. and Schindler, D.E. 2004. Effects of climatic
433 variability on the thermal properties of Lake Washington. *Limnol. Oceanogr.* **49**: 256-
434 270.
- 435 Bird, R.E. and Hulstrom, R.L. 1981. A simplified clear sky model for direct and diffuse
436 insolation on horizontal surfaces. SERI Technical Report SERI/TR-642-761, Feb 1991.
437 Solar Energy Research Institute, Golden, CO., U.S.A 46p.
- 438 Blenckner, T., Omstedt, A. and Rummukainen, M. 2002. A Swedish case study of contemporary
439 and possible future consequences of climate change on lake function. *Aquat. Sci.*
440 **64**:171184.
- 441 Brock, T.D. 1981. Calculating solar radiation for ecological studies. *Ecol. Modelling* **14**: 1-19.
- 442 Burnham, K. P., and Anderson, D. R., 2004. Multi-model inference: understanding AIC and BIC
443 in model selection. *Sociological Methods and Research* **33**: 261–304.
- 444 Bussi eres, N and Schertzer, W.M. 2003. The evolution of AVHRR-derived water temperatures
445 over lakes in the Mackenzie Basin and hydro-meteorological applications. *J.*
446 *Hydrometeorology* **4**: 660-672.
- 447 Bussi eres, N., Versegny, D. and MacPherson, J.I. 2002. The evolution of AVHRR-derived water
448 temperatures over boreal lakes. *Remote Sensing of Environment* **80**: 373-384.

Minns et al

CJFAS2017_0061 TP JP

21/06/2017

- 449 Chu, C., Minns, C.K., Lester, N.P. and Mandrak, N.E. 2015. An updated assessment of
450 freshwater fish biodiversity, the environment and human activities in Canada. *Can. J.*
451 *Fish. Aquat. Sci.* **72**(1): 135-148.
- 452 Chubarenko, I. and Hutter, K. 2005. Thermally driven interaction of littoral and limnetic zones
453 by autumnal cooling processes. *J. Limnol.* **64**(1): 31-42.
- 454 Currey, D.R. 1974. Continentality of extratropical climates. *Annals Assoc. Amer. Geographers*
455 **64**(2): 268-280.
- 456 Fairall, C.W., Bradley, E.F., Godfrey, J.S., Wick, G.A., Edson, J.B., and Young, G.S. 1996.
457 Cool-skin and warm-layer effects on sea surface temperature. *J. Geophys. Res.* **101**(C1):
458 1295-1308.
- 459 Flaim G., Eccel, E., Zeileis, A., Toller, G., Cerasino, L. and Obertegger, U. 2016. Effects of re-
460 oligotrophication and climate change on lake thermal structure. *Freshwater Biology*
461 **61**(10): 1802-14.
- 462 Gholizadeh, M.H., Melesse, A.M. and Reddi, L. 2016. A comprehensive review on water quality
463 parameter estimate using remote sensing techniques. *Sensors* **16**: 1298, 43p.
- 464 Gunn, J.M., Snucins, E., Yan, N.D. and Arts, M.T. 2001. Use of water clarity to monitor the
465 effects of climate change and other stressors in oligotrophic lakes. *Environ. Monit.*
466 *Assess.* **67**:69-88.
- 467 Håkanson, L. 1996. A new, simple, general technique to predict seasonal variability of river
468 discharge and lake temperature for lake ecosystem models. *Ecol. Modelling* **88**:157-181.
- 469 Harris, I., Jones, P.D., Osborn, T.J. and Lister, D.H. 2014, Updated high-resolution grids of
470 monthly climatic observations - the CRU TS3.10 Dataset. *Int. J. Climatol.* **34**: 623-642.
471 doi: 10.1002/joc.3711

Minns et al

CJFAS2017_0061 T_P J_P

21/06/2017

- 472 Hasnain S.S., Shuter B.J., and Minns C.K. 2013. Phylogeny influences the relationships linking
473 key ecological thermal metrics for North American freshwater fish species. *Canadian*
474 *Journal of Fisheries and Aquatic Sciences*. 70(7): 964-972.
- 475 Henderson-Sellers, B. 1986. Calculating the surface energy balance for lake and reservoir
476 modelling: a review. *Revs. Geophysics* **24**(3): 625-649.
- 477 Hondzo, M. and Stefan, H.G. 1993. Regional water temperature characteristics of lakes subjected
478 to climate change. *Climatic Change* **24**: 187-211.
- 479 Huang, A., Rao, Y.R., Lu, Y. and J. Zhao, J. 2010. Hydrodynamic modeling of Lake Ontario: An
480 inter-comparison of three models. *J. Geophys. Res.* **115**: C12076,
481 doi:10.1029/2010JC006.
- 482 Hunt, L.M., Fenichel, E.P., Fulton, D.C., Mendelsohn, R., Smith, J.W., Tunney, T.D. Lynch,
483 A.J., Paukert, C.P. and Whitney, J.E. 2016. Identifying alternate pathways for climate
484 change to impact inland recreational fishers. *Fisheries* **41**(7): 362-372.
- 485 IPCC, 2013: Climate Change 2013: The Physical Science Basis. Contribution of Working Group
486 I to the Fifth Assessment Report of the Intergovernmental Panel on Climate Change
487 [Stocker, T.F., D. Qin, G.K. Plattner, M. Tignor, S.K. Allen, J. Boschung, A. Nauels, Y.
488 Xia, V. Bex and P.M. Midgley (eds.)]. Cambridge University Press, Cambridge, United
489 Kingdom and New York, NY, USA, 1535 pp.
- 490 Kasten, F. and Czeplak, G. 1980. Solar and terrestrial radiation dependent on the amount and
491 type of cloud. *Solar Energy* 24: 177-189.
- 492 Larouche, P. and Galbraith, P.S. 2016. Canadian Coastal Seas and Great Lakes Sea Surface
493 Temperature Climatology and Recent Trends. *Can. J. Remote Sensing*, 42(3): 243-258.

Minns et al

CJFAS2017_0061 T_P J_P

21/06/2017

- 494 Latifovic, R., and Pouliot, D. 2007. Analysis of climate change impacts on lake ice phenology in
495 Canada using the historical satellite data record. *Remote Sensing of Environment* **106**:
496 492–507.
- 497 Latifovic, R., Trishchenko, A.P., Chen, J., Park, W.B., Khlopenkov, K.V., Fernandes, R.,
498 Pouliot, D., Ungureanu, C., Luo, Y., Wang, S., Davidson, A., and Cihlar, J. 2005.
499 Generating historical AVHRR 1 km baseline satellite data records over Canada suitable
500 for climate change studies. *Can. J. Remote Sensing*. **31**: 324-346.
- 501 Livingstone, D.M., Lotter, A.F. and Kettle, H. 2005. Altitude-dependent differences in the
502 primary physical response of mountain lakes to climatic forcing. *Limnol. Oceanogr.* **50**:
503 1313-1325.
- 504 Lüdecke D. 2016. *sjmisc: Miscellaneous Data Management Tools*. R package version 2.0.1,
505 <https://CRAN.R-project.org/package=sjmisc>.
- 506 Lynch, A.J., Myers, B.J., Chu, C., Eby, L.A., Falke, J.A., Kovach, R.P., Krabbenhoft, T.J.,
507 Kwak, T.J., Lyons, J., Paukert, C.P. and Whitney, J.E. 2016. Climate change effects on
508 North American inland fish populations and assemblages. *Fisheries* **41**(7): 346-361.
- 509 Minns, C.K. 2010. Limnological characteristics of Canada's poorly known large lakes *Aquatic*
510 *Ecosystem Health and Management* **13**: 107-117.
- 511 Minns, C.K. 2009. The potential future impact of climate warming and other human activities on
512 the productive capacity of Canada's lake fisheries: A meta-model *Aquatic Ecosystem*
513 *Health and Management* **12**:152-167.
- 514 Minns, C.K. and Shuter, B.J. 2013. A semi-mechanistic seasonal temperature-profile model
515 (STM) for the period of stratification in dimictic lakes. *Can. J. Fish. Aquat. Sci.* **70**(2):
516 169-181.

Minns et al

CJFAS2017_0061 T_P J_P

21/06/2017

- 517 Minns C.K., Shuter B.J., and Fung S. 2014. Regional projections of climate change effects on
518 thermal habitat space for fishes in stratified Ontario lakes. *Climate Change Research*
519 *Report-Ontario Forest Research Institute* 41: 32p.
- 520 Minns, C.K., Moore, J.E., Shuter, B.J., and Mandrak, N.E. 2008. A preliminary analysis of some
521 key characteristics of Canadian lakes. *Can. J. Fish. Aquat. Sci.* **65**: 1763-1778.
- 522 Nakagawa, S. and Schielzeth, H. 2013. A general and simple method for obtaining R^2 from
523 generalized linear mixed-effects models. *Methods in Ecology and Evolution* **4**: 133-142.
- 524 O'Reilly, C.M., Sharma, S., Gray, D.K., Hampton, S.E., et al. 2015. Rapid and highly variable
525 warming of lake surface waters around the globe, *Geophys. Res. Lett.* **42**(24): 10773-
526 10781.
- 527 Patterson, J.C., Hamblin, P.F. and Imberger, J. 1984. Classification and dynamic simulation of
528 the vertical density structure of lakes. *Limnol. Oceanogr.* **29**: 845-861.
- 529 Pinheiro, J., Bates, D., DebRoy, S., Sarkar, D. and R Core Team. 2016. *nlme: Linear and*
530 *Nonlinear Mixed Effects Models*. R package version 3.1-128,
531 <http://CRAN.Rproject.org/package=nlme>.
- 532 Prairie, Y.T. 1996. Evaluating the predictive power of regression models. *Can. J. Fish. Aquat.*
533 *Sci.* **53**: 490-492.
- 534 R Core Team. 2015. R: A language and environment for statistical computing. R Foundation for
535 Statistical Computing, Vienna, Austria. URL <https://www.R-project.org/>.
- 536 Reist J.D., Wrona, F.J., Prowse, T.D., Power, M., Dempson, J.B., et al. 2006. General effects of
537 climate change on arctic fishes and fish populations. *Ambio* **35**(7): 370–380.
- 538 Schindler, D.W. 2001. The cumulative effects of climate warming and other human stresses on
539 Canadian freshwaters in the new millennium. *Can. J. Fish. Aquat. Sci.* **58**:18-29.

Minns et al

CJFAS2017_0061 T_P J_P

21/06/2017

- 540 Schwab, D.J., Leshkovich, G.A. and Muhr, G.C. 1999. Automated mapping of surface water
541 temperatures in the Great Lakes. *Journal of Great Lakes Research* **25**: 468-481.
- 542 Sharma, S., Walker, S.C., and Jackson, D.A. 2008. Empirical modelling of lake water
543 temperature relationships: a comparison of approaches. *Freshwater Biol.* **53**: 897-911.
- 544 Sharma, S., Jackson, D.A., Minns, C.K., and Shuter, B.J. 2007. Will northern fish populations be
545 in hot water because of climate change? *Global Change Biology* **13**: 2052-2064.
- 546 Shuter, B. J., Finstad, A.G., Helland, I., Zweimüller, I.P. and Hölker, F. 2012. The role of winter
547 phenology in shaping the ecology of freshwater fish and their sensitivities to climate
548 change. *Aquatic Sciences* **74**(4): 637-657.
- 549 Shuter, B.J., Schlesinger, D.A., and Zimmerman, A.P. 1983. Empirical predictors of annual
550 surface water temperatures in North American lakes. *Can. J. Fish. Aquat. Sci.* **40**:1838-
551 1845.
- 552 Snucins, E. and Gunn, J. 2000. Inter-annual variation in the thermal structure of clear and
553 coloured lakes. *Limnol. Oceanogr.* **45**: 1639-1646.
- 554 Sprugel, D.G. 1983. Correcting for bias in log-transformed allometric equations. *Ecology* **64**(1):
555 209-210.
- 556 Stine, A.R., Huybers, P. and Fung, I.Y. 2011. Changes in the phase of the annual cycle of surface
557 temperature. *Nature*, **457**: 435–441.
- 558 Stolwijk, A.M., Straatman, H. and Zielhuis, G.A. 1999. Studying seasonality by using sine and
559 cosine functions in regression analysis. *J. Epidemiol. Community Health* **53**: 235-238.
- 560 Toffolon, M., Piccolroaz, S., Majone, B., Soja, A-M., Peeters, F., Schmid, M. and Wüest, A.
561 2014. Prediction of surface temperature in lakes with different morphology using air
562 temperature. *Limnol. Oceanogr.* **59**(6): 2185-2202.

Minns et al

CJFAS2017_0061 T_P J_P

21/06/2017

- 563 Tanentzap, A.J., Hamilton, D.P., and Yan, N.D. 2007. Calibrating the Dynamic Reservoir
564 Simulation Model (DYRESM) and filling required data gaps for one-dimensional thermal
565 profile predictions in a boreal lake. *Limnol. Oceanogr. Methods* **5**: 484-496.
- 566 Wang D., Morton D., Masek J., Wu A., Nagol J., Xiong X., Levy R., Vermote E. and Wolfe R.
567 2012. Impact of sensor degradation on the MODIS NDVI time series. *Remote Sensing of*
568 *Environment*. 119: 55-61.
- 569 Williamson, C.E., Saros, J.E., Vincent, W.F., and Smol, J.P. 2009. Lakes and reservoirs as
570 sentinels, integrators, and regulators of climate change. *Limnol. Oceanogr.* **54**(6, Pt2):
571 2273-2282.
- 572 Yin, X. 1996. Reconstructing monthly global solar radiation from air temperature and
573 precipitation records: a general algorithm for Canada. *Ecol. Modelling* **88**: 39-44.
- 574 Zuur, A.F., Iena, E.N., Walker, N.J., Saveliev, A.A., and Smith, G.M. 2009. *Mixed Effect Models*
575 *and Extensions in Ecology with R*. Springer, New York, 574p.
- 576 Appendices and Supplementary Material Available On-line:
577 Appendix A – Acquisition of Remotely Sensed (RS) data
578 Appendix B - Skin to bulk adjustment of RS temperatures using GLSEA data
579 Supplementary Material
- 580

581 Table 1. The best fit LME models for estimates of peak summer surface temperature (T_P) and its
 582 date of occurrence (J_P) obtained with the usable dataset (N=690) starting with 3 lake variables
 583 and 15 climate variables. Significance level for probability is <0.01 except for P_{ANN} in the T_P
 584 model (*, P=0.0175)
 585

Element	T _P Coefficients		J _P Coefficients	
<i>Random effects</i>				
	<i>S.D.</i>		<i>S.D.</i>	
Model	0.727		4.326	
Lake/Model	1.194		4.354	
Residual	0.850		3.882	
<i>Fixed effects</i>				
	<i>Estimate</i>	<i>S.E.</i>	<i>Estimate</i>	<i>S.E.</i>
Intercept	46.030	5.260	439.187	37.465
Ln (Area)	-1.758	0.119	5.503	0.435
Ln (Peri)	1.459	0.166	-4.980	0.610
Ln (Elev+1)	-0.310	0.090	-	-
T _{JUL}	0.282	0.044	0.850	0.307
T _{SUM}			-1.034	0.357
T _{ANN}	0.373	0.031		
P _{ANN}	-0.463	0.194 *		
C _{JUL}	-0.066	0.014		
C _{ANN}	-0.160	0.030		
R _{ANN}			-0.321	0.066
R _{RGE}	-0.040	0.012	-0.566	0.082
<i>Statistics</i>				
R ² Marginal	0.742		0.286	
R ² Conditional	0.930		0.796	
AICc	2424.430		4336.770	

586 6

587 7

588
589
590
591
592
593
594
595
596
597
598
599
600
601
602
603
604
605
606

List of Figures

Figure 1. Map showing the location and size ranges of Canada's large lakes (Area $\geq 100 \text{ km}^2$).

Figure 2. Plots of adjusted RS bulk temperatures versus day of year for nine lake datasets that passed our quality control criteria. Predicted curves are given for the best sinusoidal (solid line) model and for fitted quadratic (dotted line), and the breakpoint (dashed line) models (See Supplementary Table S1 for more information about the lakes and their selection).

Figure 3. Univariate plots of T_P estimates against the climate metrics (mean July (JUL), summer (SUM), and annual (ANN) air temperature (T), total precipitation (P), and cloud cover (C), and mean July (JUL), range of monthly means (RGE), and annual (ANN) clear-sky (R) and cloud corrected solar radiation (CR).

Figure 4. Univariate plots of T_P estimates against the lake metrics (ln area, ln perimeter, ln (elevation+1), ln maximum depth, ln mean depth, ln Secchi depth) and latitude and longitude.

Figure 5. Comparisons of T_P estimates obtained here with the values predicted using the models of (A) Shuter et al. 1983 (model 10 in their Table 4) and (B) Sharma et al. 2007 (the average of predictions for models 1 and 2).

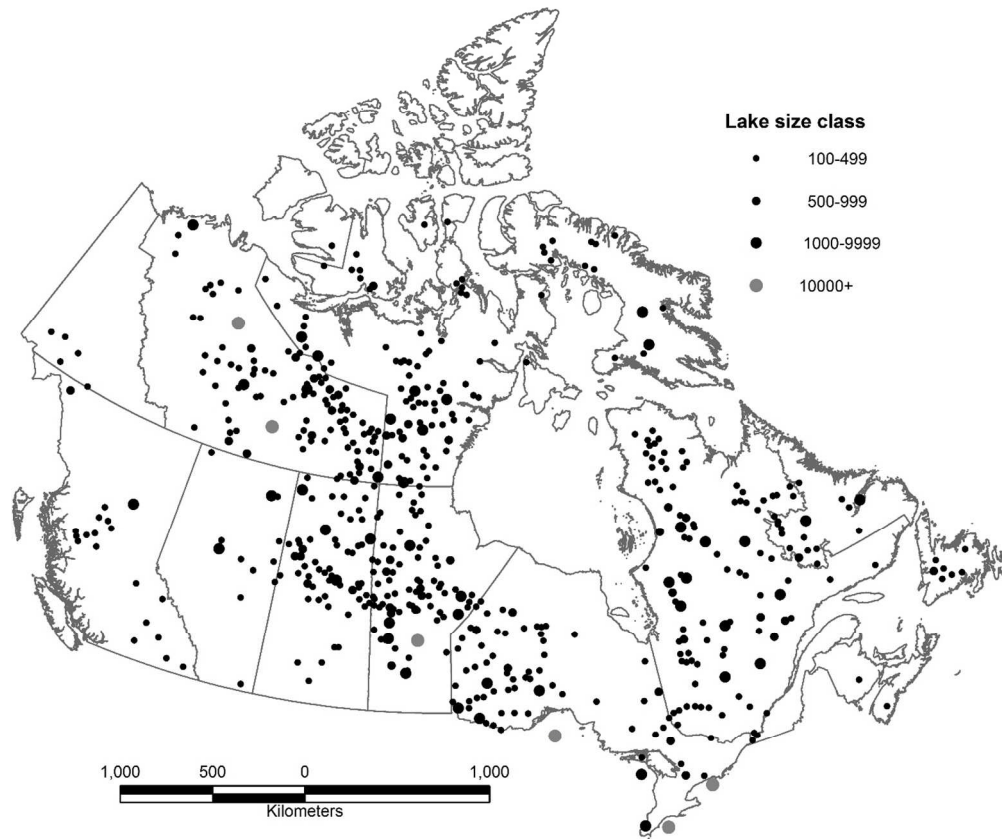


Figure 1. Map showing the location and size ranges of Canada's large lakes (Area ≥ 100 km²).

164x137mm (220 x 220 DPI)

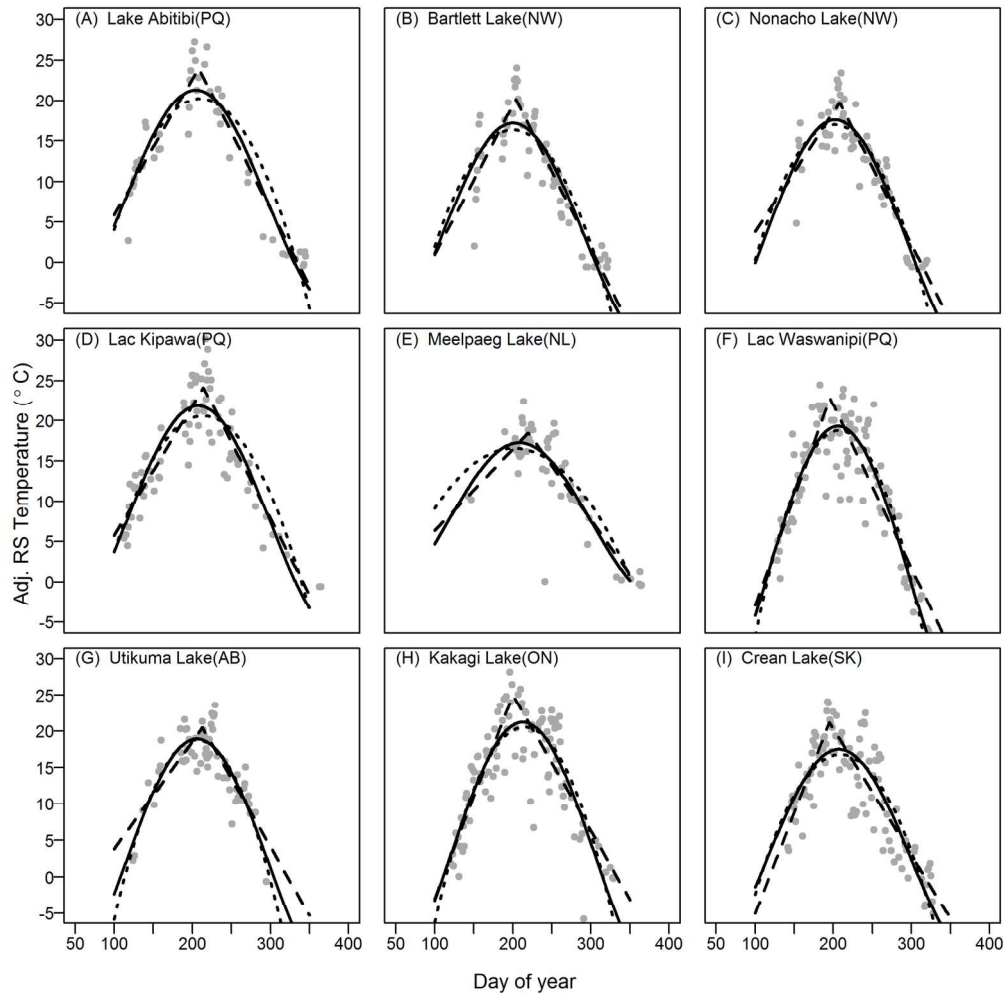


Figure 2. Plots of adjusted RS bulk temperatures versus day of year for nine lake datasets that passed our quality control criteria. Predicted curves are given for the best sinusoidal (solid line) model and for fitted quadratic (dotted line), and the breakpoint (dashed line) models (See Supplement Table S1 for more information about the lakes and their selection).

165x165mm (300 x 300 DPI)

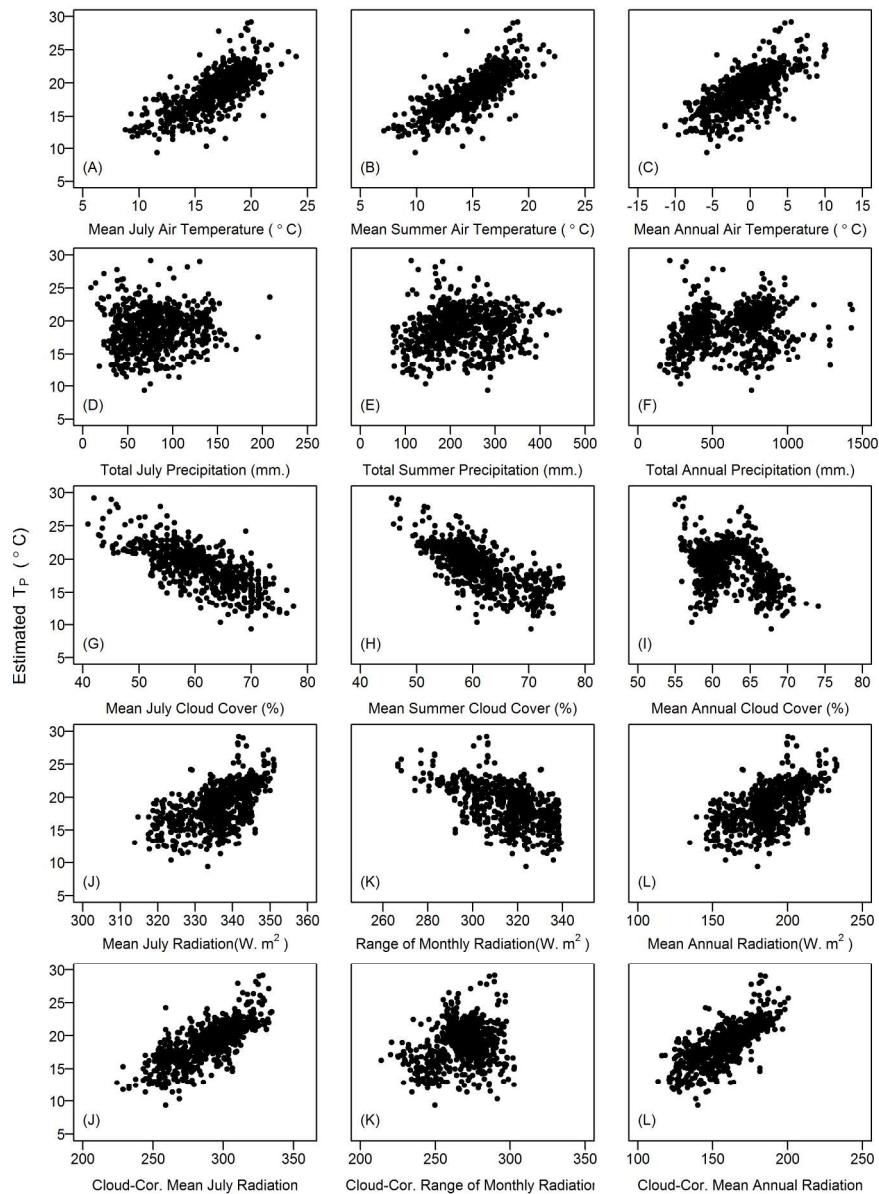


Figure 3. Univariate plots of TP estimates against the climate metrics (mean July (JUL), summer (SUM), and annual (ANN) air temperature (T), total precipitation (P), and cloud cover (C), and mean July (JUL), range of monthly means (RGE), and annual (ANN) clear-sky (R) and cloud corrected solar radiation (CR).

228x316mm (300 x 300 DPI)

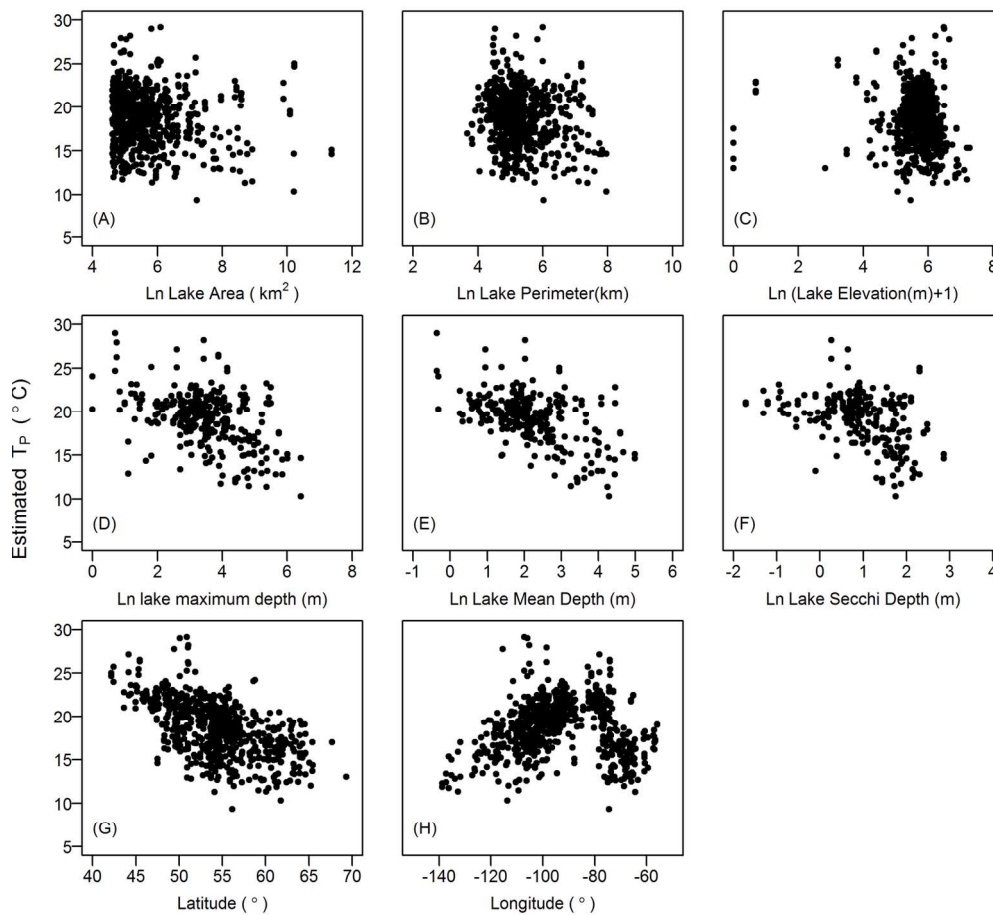


Figure 4. Univariate plots of TP estimates against the lake metrics (ln area, ln perimeter, ln (elevation+1), ln maximum depth, ln mean depth, ln Secchi depth) and latitude and longitude.

152x140mm (300 x 300 DPI)

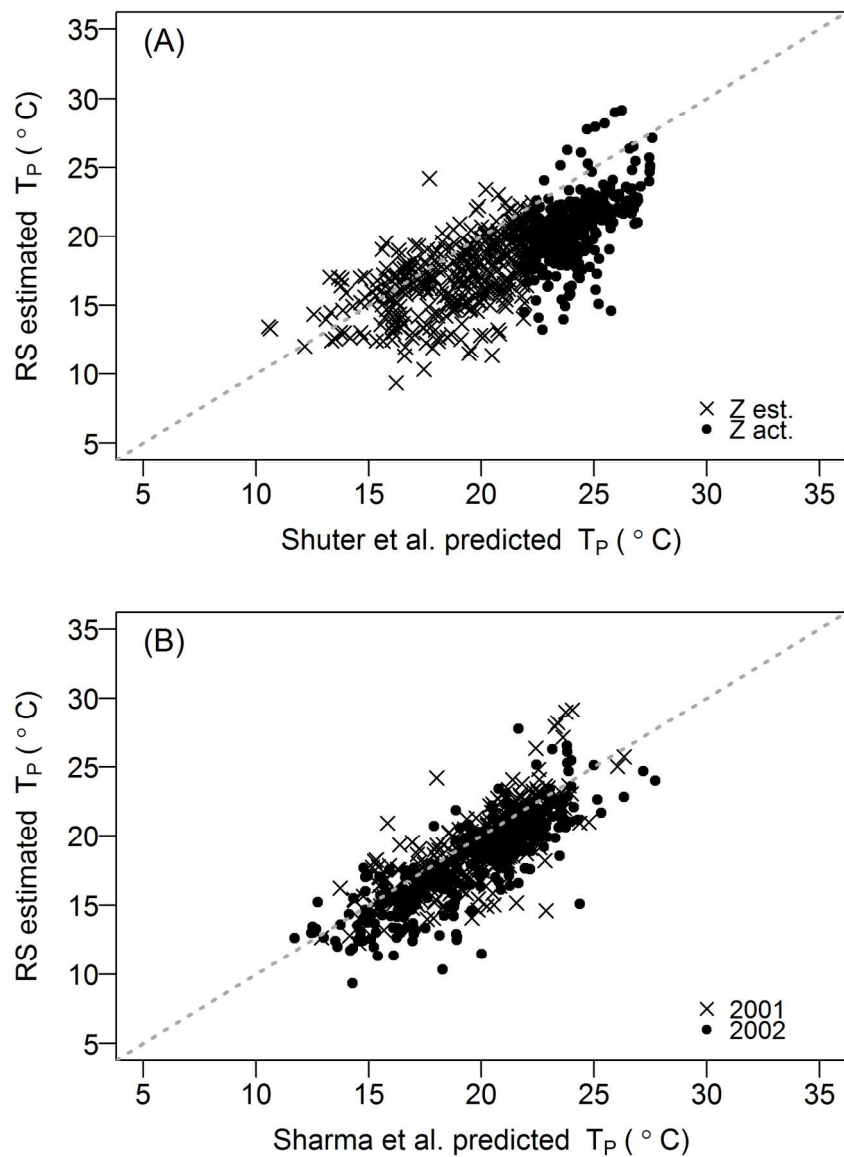


Figure 5. Comparisons of TP estimates obtained here with the values predicted using the models of (A) Shuter et al. 1983 (model 10 in their Table 4) and (B) Sharma et al. 2007 (the average of predictions for models 1 and 2).

177x248mm (300 x 300 DPI)

1 **Appendix A – Acquisition of Remotely Sensed (RS) Data**

2 *MODIS/Terra Land Surface Temperature (MOD11A1) and Albedo (MOD43B3) Data*

3 MODIS (Moderate Resolution Imaging Spectro-radiometer) on the Terra (EOS AM)
4 satellite is a remote sensing instrument operated by NASA since 1999 and provides complete
5 coverage of the earth every 1 to 2 days. The MODIS Land Surface Temperature and Emissivity
6 (LST/E) product (MOD11A1; version Level (collection) 4) provides daytime and night-time per-
7 pixel temperature and emissivity values at 1km spatial (pixel) resolution; MODIS/Terra data
8 were used rather than the MODIS Aqua data since the national composites using these data had
9 already been downloaded and processed by CCRS and the project only had resources to work
10 with available datasets. The best quality retrievals from this process can yield 1 °K accuracy for
11 materials with known emissivities.

12 The MODIS Bidirectional Reflectance Distribution Function (BRDF; Wanner et al 1997;
13 Schaaf et al 2002) was used to compute a global set of parameters describing the BRDF of the
14 land surface. These parameters described the BRDF of each 1-km pixel in MODIS bands 1– 7
15 (product MOD43B1). The MODIS albedo product (product MOD43B3) generated black-sky
16 (direct radiation) and white-sky (diffuse radiation) albedo datasets for each of these seven bands
17 and for the visible, near infrared, and total shortwave broadbands (0.3–0.7, 0.7–5.0, and 0.3–5.0
18 μm , respectively) (Schaaf et al. 2002). Broadband albedos are calculated using spectral-to
19 broadband conversion algorithms (Liang 2000; Liang 2004). The MODIS albedos represent the
20 best quality data possible for each 16-day period (Zhou et al 2003). Actual (blue-sky) albedos
21 can be calculated from a linear combination of black- and white-sky albedos, depending on the
22 fraction of diffuse sunlight. Details and downloads of the MODIS LST and Albedo products are

23 available at the US Geological Survey's Land Processes Distributed Active Archive Center (LP-
24 DAAC).

25 The MODIS LST and Albedo data were mosaicked and re-projected using the MODIS
26 reprojection tool (version 3.1, US Geological Survey 2003) to a Lambert Conformal Conic
27 (LCC) with a spatial resolution of 1 km. The albedo product was used to identify islands in lakes
28 to allow exclusion of terrestrial pixels from the computation of the lake-wide mean skin
29 temperatures (see National Lake Cover Map section below).

30 For each day that MODIS data were available, two average lake kinetic temperatures
31 (day-time; night-time) were extracted from MODIS observations. To do this, the pixels
32 corresponding to each unique lake ID in the Canadian National Lake Cover Map (see below)
33 were matched to their corresponding pixels in the MODIS temperature data. The pixels used in
34 the calculation of average lake skin temperature for a given lake of interest were those that
35 matched the unique lake ID of the lake of interest. We used the quality assurance (QA) science
36 datasets (SDs) distributed with the MOD11A1 data product to select and use only the LST pixel
37 observations that were considered "best quality" (i.e. the "QC_day" and "QC_night" SDs).
38 However, in some cases, where the application of these criteria yielded no or few good
39 observations, we relaxed these criteria to also include LST retrievals whose quality was less
40 certain. This process is described in detail, below. The "QC_day" and "QC_night" SDs are
41 available as 8-bit images, in which successive pairs of bit-flags correspond to various aspects of
42 data quality. The four possible combinations of any given bit-flag (i.e. 00, 10, 01, 11) are used to
43 denote data of varying quality, and thus, can be used to quality assure the data to the level
44 required by the investigator. Initially, we selected only the LST retrievals for day and night that
45 were considered to be of the highest quality (bits 1&0 =00; "LST produced, good quality, not

46 necessary to examine more detailed QA"). The average LST error associated with data flagged
47 with this combination is estimated as $\leq 1\text{K}$ (bits 7&6=00; "Average LST error $\leq 1\text{K}$ ") (see
48 MOD11A1 ATBD for details). However, in some cases, we found that this QA approach was too
49 restrictive, and yielded few pixels of good quality over some lakes. To address this problem, we
50 relaxed our QA criteria over such lakes so that "acceptable" retrieval values were defined where
51 bits 1&0 =01; "LST produced, other quality, recommend examination of more detailed QA" and
52 where bits 7&6=01; "Average LST error $\leq 2\text{K}$ "). After the QA process, we only retained the
53 MODIS daytime retrievals for this study, with a stated accuracy of $\leq 2\text{ }^\circ\text{K}$, and, then, only when
54 average lake skin temperatures were based on the mean for cloud-free pixels representing at least
55 65% of the lake area. The 65% value was an arbitrary threshold selected to ensure a
56 representative estimate of the lake-wide mean skin temperature.

57 *AVHRR Ice dates*

58 Concurrent with the analysis of the MODIS data, AVHRR remote sensing data was
59 processed using the protocol of Latifovic and Pouliot (2007) to determine ice break-up and
60 freeze-up dates in the Canadian large lakes. Only daytime MODIS data from the period between
61 the end of break-up and the completion of freeze-up in each lake and year were used in this
62 study.

63 *National Lake Cover Map (Lake Mask)*

64 The national lake cover map was created from a national 1:1million scale vector spatial
65 dataset that contained all of Canada's mapped lakes and reservoirs. Canadian lakes and
66 reservoirs with surface areas $\geq 100\text{ km}^2$ were extracted from this dataset, creating a vector lake
67 cover map containing 563 lakes and reservoirs. To make this map consistent with the rest of our
68 satellite data, it was re-projected to the LCC projection, then converted to a raster grid of 1km

69 spatial resolution. A raster lake dataset was created during this process where pixels were
70 assigned a value of 0 (land) or > 0 (water). In this dataset, water pixel values corresponded to a
71 unique lake ID that matched the lake IDs recorded in an additional non-spatial dataset (Demers
72 1975). This numbering system facilitated the extraction of lake-specific information from the
73 satellite data and allowed each lake in the spatial data base to be easily cross-referenced with
74 other information (e.g. lake physical characteristics).

75 The geometric fidelity of the lake cover raster dataset was then compared to other
76 available raster (e.g. MODIS) and vector (e.g. lake and coastline) datasets. A visual analysis was
77 done to make sure that the registration error was low (i.e. $< one or two pixels$). A subsample of
78 lakes across the country were chosen (not random, but some from north, south, east and west) to
79 see how well the vector layer matched up with the raster layers. Of interest to us were (i) ability
80 to accurately map the lake shoreline and (ii) ability to accurately map lake islands (which would
81 subsequently be masked from the remote sensing analysis). No significant problems were found.
82 This analysis showed that an acceptable and consistent level of geo-referencing accuracy was
83 maintained across all Canadian lakes.

84 The quality control of the lake dataset also included the identification and elimination of
85 lake islands that were not included in the original lake vector dataset. These island (non-water)
86 pixels were identified on the basis of their annual maximum and minimum MODIS VIS and NIR
87 albedo values (e.g. water frozen all year round: $VIS_{min} > 0.7$; Lakes frozen in winter but not
88 frozen in summer: $VIS_{max} > 0.7$ and $NIR_{min} < 0.05$; Lakes never frozen: $NIR_{max} < 0.05$). These
89 criteria were used because they consider the full annual variation in lake surface albedo typical
90 of water bodies. Where missing (i.e. MODIS data left a pixel's cover class uncertain), the
91 AVHRR archive described by Latifovic et al (2005) was used to define land and water pixels.

92 The Canadian lake mask identified 563 large lakes (Figure 1; Minns et al 2008) although there
93 were some lakes (<10) that did not appear in the Canadian Survey on the Water Balance of
94 Lakes (CSWBL) (Demers 1975). This discrepancy was thought to be due to errors arising from
95 the misclassifying of water bodies when earlier gridded map sheets were digitized, before remote
96 sensing coverage was available and geographic information systems came into wide use.

97 *References*

- 98 Demers, J. (ed.). 1975. Canadian Survey on the water balance of lakes. Secretariat Canadian
99 National Comm. Internat. Hydrol. Decade (1965-1975). Environment Canada, Can. Govt.
100 Publishing Report, 92p. (On file in the library of the Canada Centre for Inland Waters,
101 Burlington, Ontario).
- 102 Latifovic, R., and Pouliot, D. 2007. Analysis of climate change impacts on lake ice phenology in
103 Canada using the historical satellite data record. *Remote Sensing of Environment* **106**:
104 492–507.
- 105 Latifovic, R., Trishchenko, A.P., Chen, J., Park, W.B., Khlopenkov, K. V., Fernandes, R.,
106 Pouliot, D., Ungureanu, C., Luo, Y., Wang, S., Davidson, A., and Cihlar, J. 2005.
107 Generating historical AVHRR 1 km baseline satellite data records over Canada suitable
108 for climate change studies. *Can. J. Remote Sensing*. **31**: 324-346.
- 109 Liang, S. 2000. Narrowband to broadband conversions of land surface albedo I. Algorithms.
110 *Remote Sensing of Environment* **76**: 213-238.
- 111 Liang, S. 2004. Estimation of Surface Radiation Budget: I. Broadband Albedo. In *Quantitative*
112 *Remote Sensing of Land Surfaces*, edited, John Wiley and Sons, Inc., Hoboken, New
113 Jersey, USA.

- 114 Minns, C.K., Moore, J.E., Shuter, B.J., and Mandrak, N.E. 2008. A preliminary analysis of some
115 key characteristics of Canadian lakes. *Can. J. Fish. Aquat. Sci.* **65**: 1763-1778.
- 116 Schaaf, C.B., F. Gao, F., Strahler, A.H., Lucht, W., Li, X., Tsang, T., Strugnell, N. C., Zhang, X.,
117 Jin, Y., Muller, J.-P., Lewis, P., Barnsley, M., Hobson, P., Disney, M., Roberts, G.,
118 Dunderdale, M., Doll, C., d'Entremont, R., Hu, B., Liang, S., and Privette, J. L. 2002.
119 First operational BRDF, albedo nadir reflectance products from MODIS. *Remote Sensing*
120 *of Environment* **83**: 135-148.
- 121 Wanner, W., Strahler, A.H., Hu, B., Lewis, P., Muller, J.-P., Li, X., Schaaf, C.B., and Barnsley,
122 M.J. 1997. Global retrieval of bidirectional reflectance and albedo over land from EOS
123 MODIS and MISR data: Theory and algorithm. *J. Geophys. Res.* **102**: 17143-17161.
- 124 Zhou, L., Dickinson, R.E., Tian, Y., Zeng, X., Dai, Y., Yang, Z-L., Schaaf, C.B., Gao, F., Jin, Y.,
125 Strahler, A.H., Myeni, R.B., Yu, H., Wu, W., and Shaikh, M. 2003. Comparison of
126 seasonal and spatial variations of albedos from Moderate-Resolution Imaging
127 Spectroradiometer (MODIS) and Common Land Model. *J. Geophys. Res.* **108**: 4488-
128 4688.

1 **Appendix B. Skin to bulk adjustment of RS temperatures using GLSEA data.**

2 *Introduction*

3 On the St. Lawrence, Great Lakes, NOAA (GLSEA) used a combination of remotely
4 sensed and continuous *in situ* monitoring data to obtain daily lake-wide mean bulk surface
5 temperatures for each of the Great Lakes (Schwab et al. 1999). For the four Great Lakes
6 (Superior, Huron, Erie, and Ontario) included in our RS dataset, we compared our lake-wide
7 mean skin temperatures with GLSEA bulk temperatures for the dates in the open water period
8 when we had observations.

9 *Materials and Methods*

10 Linear mixed effects modelling (LME) using maximum likelihood (lme4 R package,
11 Bates et al 2015) was used to estimate skin-to-bulk temperature adjustments. Final estimates for
12 daily bulk temperatures were obtained by applying the best adjustment model to all usable open-
13 water RS skin temperatures.

14 Prior to analyzing all the datasets, we modelled the eight Great Lakes datasets (four lakes
15 in two years). We compared the sinusoidal models with the quadratic and break-point models.
16 We also compared models fit using our adjusted RS data with models fit to an open water subset
17 of the GLSEA data selected using our ice-out/-in dates, and a further subset of those open water
18 GLSEA data whose dates matched those in our RS datasets.

19 *Results*

20 Adjustment model using Great Lakes Observations: The available RS lake-wide mean
21 skin temperatures for 2001-2002 for four Great Lakes were matched by day of year with the
22 GLSEA-estimated lake-wide mean bulk surface temperatures (Appendix Figure B1) and most
23 points were located close to the 1:1 line; The RS data showed much more variability, particularly

24 in mid-summer relative to the GLSEA bulk values which were estimated using a combination of
25 temporally-smoothed RS observations and *in situ* bulk data from a series of thermographs
26 moored offshore in the Great Lakes (Schwab et al 1999). LME modelling of GLSEA bulk
27 temperatures with 1st to 4th order polynomials of RS skin temperatures with Lake and Year as
28 random effects yielded a significant 3rd order model (R^2 marginal and conditional values of 0.890
29 and 0.913 respectively; see Table S1 for model details and results) but the resulting model
30 predicted increasing values at the low end of the RS skin temperature range and decreasing
31 values at the high end. A quadratic model produced more consistent predictions with little
32 change in the fit but the data indicated a difference between years in the placement of the
33 quadratic relationship. Finally, a quadratic model with year interactions produced an improved fit
34 (R^2 marginal 0.897 conditional 0.901; Table B1 model 4). With the Great Lakes datasets,
35 adjusted-RS values (i.e., bulk temperatures predicted from this model) tracked the seasonal
36 pattern in the GLSEA-estimates (Figure B1). The median (adjusted RS – skin RS) difference was
37 +0.91 °C with the 10th and 90th percentiles at -1.02 and +1.92 °C respectively while the median
38 (GLSEA bulk – adjusted RS) difference was +0.23 °C with the 10th and 90th percentiles at -2.82
39 and +2.57 °C respectively. The year-specific quadratic models were applied to all our RS lake-
40 wide mean skin temperature values to generate adjusted, or bulk, surface temperatures for all
41 open water observations from all lakes in 2001 and 2002.

42 Seasonal Model Selection using Great Lakes Observations: The Great Lakes datasets
43 were used to illustrate the selection of a best fit seasonal sinusoidal model and to compare with
44 the previously-used quadratic and break-point models. In the Canadian Great Lakes, we assessed
45 the impact of data source on T_p and J_p estimates using three temperature datasets that were
46 available for each of four lakes in 2001 and 2002: the GLSEA-bulk values for the whole of the

47 open-water period; the GLSEA-bulk temperatures for those days when our RS data were
48 available during open-water; and our adjusted RS data.

49 Despite the greater variability in our adjusted RS data, the best sinusoidal model fits were
50 highly significant (R^2 ranged from 0.83 to 0.99) although slightly lower compared to fits for the
51 GLSEA open-water data (A, 0.94 to 0.99) and to fits with GLSEA open-water data that was
52 coincident with our RS data (B, 0.94 to 0.99) (Table B2). With our adjusted RS values, the best
53 sinusoidal model was the 2nd order in 6 cases and 3rd order in 2 cases with R^2 ranging from 0.84
54 to 0.96 although overall the break-point model was best for Lake Huron in 2001 when the usual
55 pattern of fluctuations around a plateau in midsummer was absent (Figure B2). The best fit
56 sinusoidal models were used to estimate T_p and J_p . The T_p differences between those based on
57 GLSEA open water estimates and those based on adjusted RS estimates ranged from -2.1 to 1.6
58 C with a mean of -0.1 °C while J_p differences ranged from -5.6 to +8.2 with a mean of 2.5 days
59 (Table S3). These differences were similar to those obtained when comparing estimates obtained
60 with all the open water GLSEA data and only the GLSEA on the dates for our adjusted RS
61 values.

62 *Discussion*

63 The RS data used in this study were processed using standardized procedures to obtain
64 lake-wide mean skin temperatures during the open-water period. Those temperatures must be
65 adjusted for skin versus bulk differences. Studies typically use *in situ* bulk observations to adjust
66 the RS data (Kay et al 2005; Schwab et al 1999) but that was not feasible given the large number
67 of lakes spread across Canada in this study. The fitted skin-to-bulk quadratic regression model
68 for the GLSEA Great Lakes data gave small upward adjustments [Median (adj. RS – skin RS) =

69 0.91 °C, median (GLSEA bulk – adj. RS) = 0.23 °C] consistent with expectations in the Great
70 Lakes (Moukomla and Blanken 2016). Our RS skin temperatures showed considerably more
71 temporal variability than the GLSEA temperatures which are derived from a smoothed mixture
72 of RS and *in situ* observations. In Lake Tahoe, Wilson *et al* (2013) showed that skin
73 temperatures vary considerably diurnally, especially with wind speed and to a lesser extent with
74 atmospheric humidity and the differences between air and bulk surface water temperatures. In
75 addition, some variability in our lake-wide mean RS skin temperatures may be due to spatial
76 variation in surface temperatures within lakes (e.g. Moukomla and Blanken 2016), combined
77 with the variable levels of lake coverage on each observation day due to cloud cover and other
78 factors. For this study, an ideal adjustment scheme would have required concurrent *in situ* bulk
79 surface temperature observations at sites from a subset of the large lakes, chosen to span their
80 size and geographic ranges instead of relying solely on the Great Lakes which are the largest
81 lakes and sit at the southern part of Canada.

82 *References*

- 83 Bates, D., Maechler, M., Bolker, B. and Walker, S. 2015. Fitting Linear Mixed-Effects Models
84 Using lme4. *Journal of Statistical Software*, **67**(1): 1-48.
- 85 Kay, J.E., Kampf, S.K., Handcock, R.N., Cherkauer, K.A., Gillespie, A.R. and Burges, S.J. 2005.
86 Accuracy of lake and stream temperatures estimated from thermal infrared images. *J.*
87 *Amer. Wat. Res. Assoc.* **41**: 1161-1175.
- 88 Moukomla, S., and Blanken, P. D. 2016. Remote Sensing of the North American Laurentian
89 Great Lakes' Surface Temperature. *Remote Sensing* **8**(4): 286 15p.
- 90 Schwab, D.J., Leshkovich, G.A. and Muhr, G.C. 1999. Automated mapping of surface water
91 temperatures in the Great Lakes. *Journal of Great Lakes Research* **25**: 468-481.

92 Wilson, R.C., Hook, S.J., Schneider, P. and Schladow, S.G. 2013. Skin and bulk temperature
93 difference at Lake Tahoe: A case study on lake skin effect. *J. Geophys. Res.:*
94 *Atmospheres* **118**(18): 10332-10346.

95

96

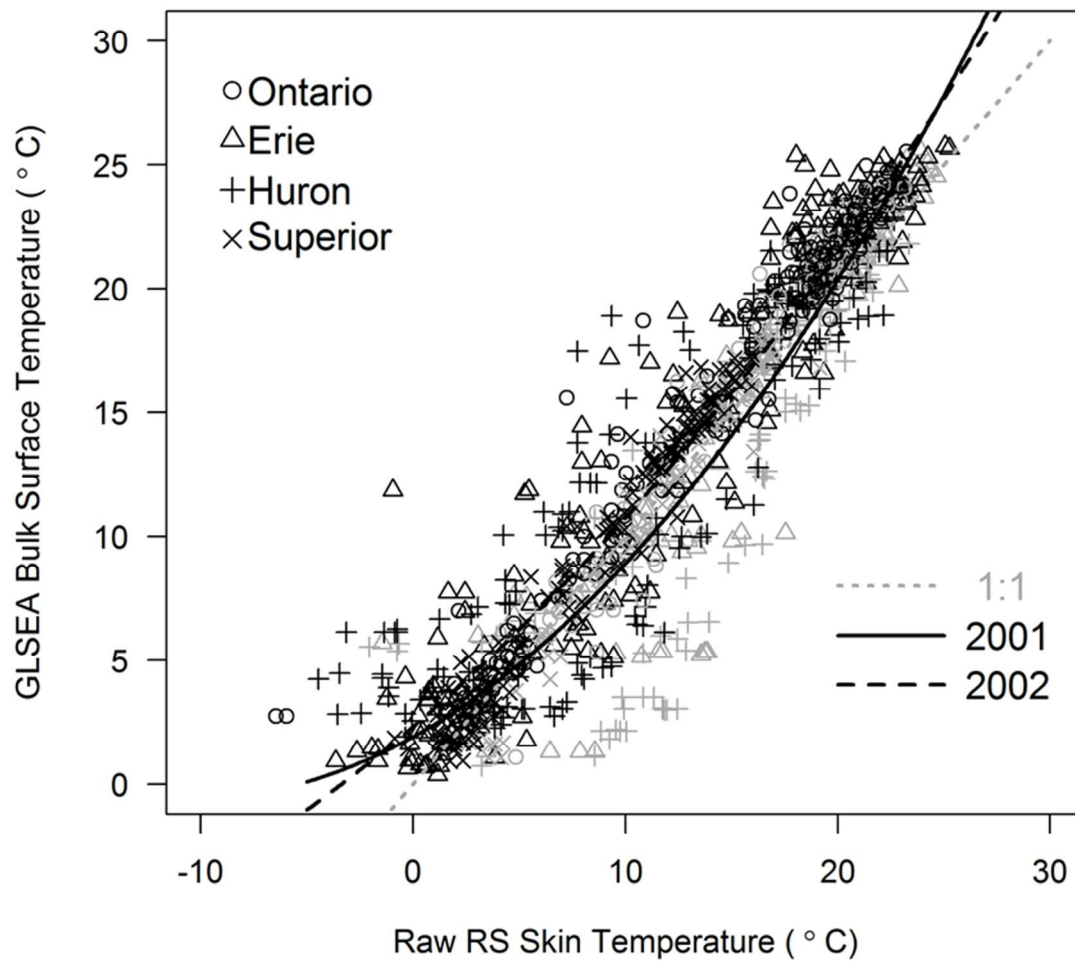
97

98

99

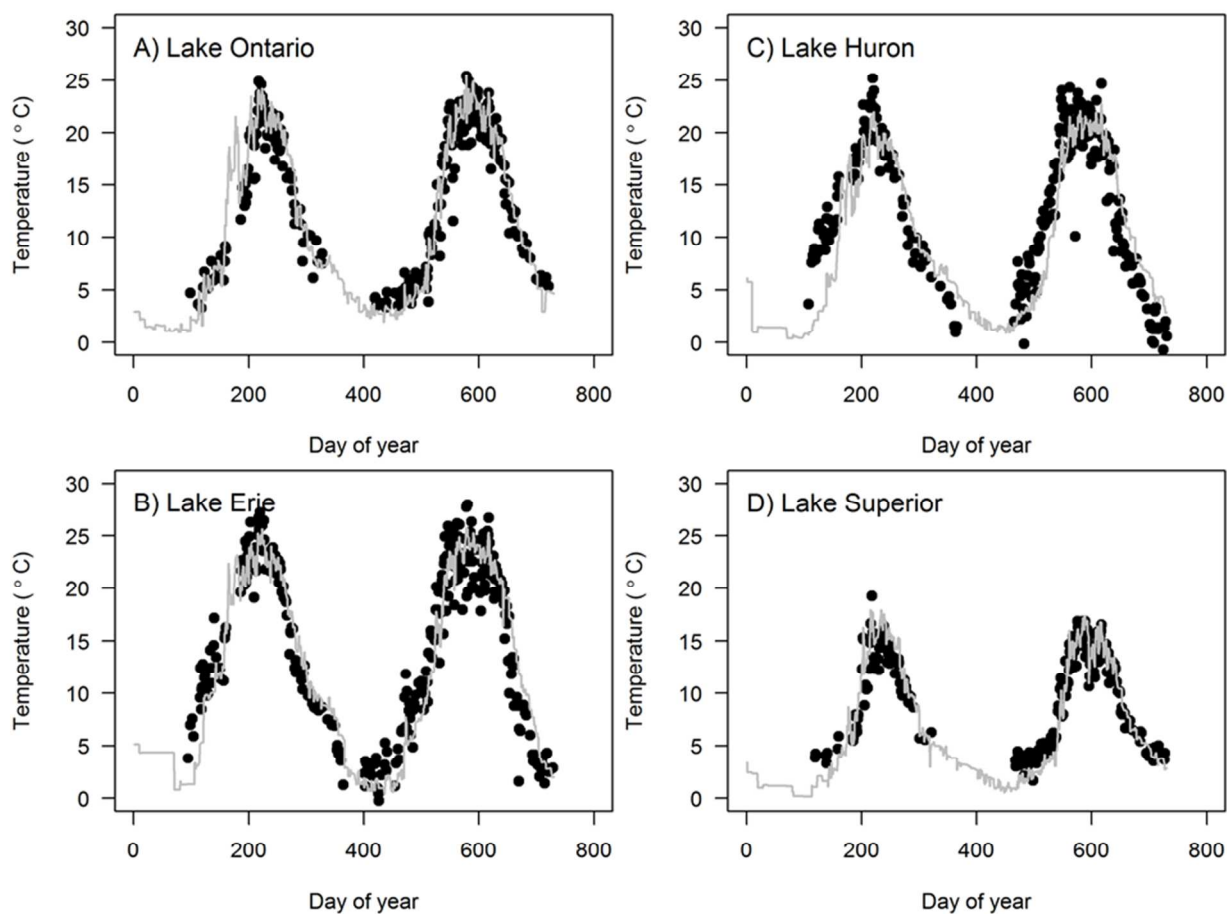
Draft

100 Figure B1. A plot of raw RS-derived lake-wide open-water mean skin temperatures ($^{\circ}\text{C}$) versus
101 GLSEA-estimated lake-wide mean bulk surface temperatures ($^{\circ}\text{C}$) across four Canadian
102 Great Lakes (Ontario, Erie, Huron and Superior) in 2001 and 2002 with a 1:1 dashed line.
103 The fitted year-specific quadratic curves (N=1096,) are shown in black (2001 - solid line,
104 2002 – dashed line).



105

106 Figure B2. Plots of the daily GLSEA lake-wide mean bulk surface temperatures in 2001 and
107 2002 (continuous grey line versus day of year with a 365-day offset for 2002 data) and of
108 the adjusted CCRS temperatures in 2001 and 2002 (black points) for: (A) Lake Ontario,
109 (B) Lake Erie, (C) Lake Huron and (D) Lake Superior.
110



111 Table B1. Comparison of results for linear mixed effects maximum likelihood models estimating GLSEA bulk surface temperatures
 112 from RS skin surface temperatures.

113

114

Model	Description	Coefficients					Residual S.D.	Mixed effects (S.D.) Lake	Year	R ²		AICc
		β_0	β_1	β_2	β_3	β_4				Marginal	Conditional	
1	4th order polynomial+ Lake and Year effects	2.239	0.163	0.0745	-0.00166	-0.0000058	2.224	0.551	0.997	0.890	0.913	4943.24
2	Best fit polynomial + Lake and Year effects	2.222	0.157	0.0773	-0.0019	na	2.223	0.550	1.000	0.890	0.913	4921.68
3	2nd order polynomial+ Lake and Year effects	1.766	0.66	0.015	na	na	2.320	0.232	0.981	0.883	0.905	4998.46
4	2nd order polynomial*Year interactions + Lake effect:						2.312	0.226	na	0.897	0.901	5003.78
	2001&2002	1.909	0.476	0.0224	na	na						
	2002 only	0.407	0.252	-0.0109	na	na						

115

116 Table B2. Results of sinusoidal model selection to allow estimation of peak summer temperature (T_p) and its date of occurrence (J_p) in
 117 four Great Lakes in 2001-2002 using: (A) All open water GLSEA bulk values; (B) GLSEA bulk values for the dates matching the
 118 available RS dates; and (C) our adjusted RS surface temperatures. *

119

Lake	Year	N	Min. AICc	AIC _c difference relative to best model fit						Best S Model	R ²	Best S Estimates		Δ vs group (A)	
				S1	S2	S3	S4	QD	BP			J _p	T _p	ΔJ _p	ΔT _p
(A) GLSEA all open-water values															
Erie	2001	274	934.7	243.8	11.5	0.0	16.4	347.1	119.9	3	0.971	221.2	23.9		
Erie	2002	331	995.2	320.4	51.5	2.7	0.0	870.2	491.9	4	0.989	216.4	24.5		
Huron	2001	261	908.5	237.9	0.0	21.4	35.1	318.0	84.1	2	0.954	224.6	19.9		
Huron	2002	268	734.1	381.1	85.4	77.0	0.0	549.3	308.3	4	0.987	220.3	21.1		
Ontario	2001	274	1102.2	182.8	0.0	13.7	28.1	291.1	88.9	2	0.938	224.9	22.3		
Ontario	2002	327	1009.6	501.1	37.9	21.6	0.0	865.8	555.3	4	0.984	218.3	23.1		
Superior	2001	257	720.7	405.5	71.8	0.0	22.8	501.7	259.8	3	0.972	237.3	16.7		
Superior	2002	264	823.3	310.8	50.8	35.4	0.0	420.3	236.8	4	0.965	225.2	15.8		
(B) GLSEA open-water on group (C) dates only															
Erie	2001	122	400.5	92.0	16.5	0.0	34.6	154.4	30.8	3	0.981	226.0	24.1	4.7	0.2
Erie	2002	198	656.5	132.3	23.9	1.2	0.0	454.6	241.9	4	0.987	213.9	24.5	-2.5	-0.1
Huron	2001	103	334.0	117.9	0.0	12.4	45.7	158.2	19.6	2	0.975	229.3	20.0	4.8	0.1
Huron	2002	171	524.0	178.7	29.7	29.7	0.0	281.1	153.8	4	0.986	221.2	21.0	1.0	0.0
Ontario	2001	102	377.7	43.5	0.0	9.0	32.1	88.7	5.9	2	0.959	231.2	22.3	6.4	0.1
Ontario	2002	165	579.9	183.5	0.0	8.4	6.4	358.0	203.1	2	0.973	226.6	23.8	8.4	0.6
Superior	2001	77	280.2	54.5	0.0	15.8	45.7	78.5	19.3	2	0.939	236.9	16.5	-0.4	-0.2
Superior	2002	158	566.6	115.3	0.0	10.3	6.5	185.6	95.2	2	0.944	234.7	16.0	9.6	0.2
												Mean		4.0	0.1
(C) Our adjusted RS surface temperatures															
Erie	2001	122	492.5	44.3	14.5	0.0	30.4	108.7	5.8	3	0.957	223.0	25.0	1.7	1.2
Erie	2002	198	929.7	38.6	0.0	18.1	22.0	190.7	68.4	2	0.923	220.9	24.7	4.5	0.1
Huron	2001	103	395.5	51.2	35.1	31.3	63.4	100.8	0.0	6	0.930	218.9	21.5	-5.6	1.6
Huron	2002	171	781.1	20.2	0.0	24.0	50.1	91.6	34.7	2	0.914	219.2	21.7	-1.1	0.6
Ontario	2001	102	428.8	50.1	0.0	6.8	36.6	81.6	10.1	2	0.921	230.8	21.0	5.9	-1.3
Ontario	2002	165	723.6	83.3	0.0	23.1	40.5	211.3	88.0	2	0.928	226.5	22.8	8.2	-0.3
Superior	2001	77	322.2	26.9	0.0	21.1	54.0	40.4	5.4	2	0.832	236.6	14.6	-0.7	-2.1
Superior	2002	158	556.9	102.1	0.0	22.1	41.6	160.6	81.3	2	0.923	232.5	15.1	7.4	-0.7
												Mean		2.5	-0.1

120 *Doy is Day of year; Min.AC AICc is the minimum among the 4 sinusoidal models (S1-S4); QD is quadratic model; BP is breakpoint model; R² is the adjusted
 121 index of determination; ΔT_p and ΔJ_p are the differences from (A) estimates. Positive AICc differences indicate that model is not as predictive as the best model.